Fracture Behavior of Carbon Fiber Reinforced Plastics Determined by the Time–Frequency Analysis Method

Ki-Woo Nam, Seok-Hwan Ahn, Chang-Kwon Moon

College of Engineering, Pukyong National University, 100, Yongdang-dong, Nam-gu, Busan, 608-739, Korea

Received 25 February 2002; revised 21 June 2002; accepted 21 June 2002

ABSTRACT: Fourier transform has been used to study the frequency characteristics of a signal. However, based on the Fourier transform and power spectrum alone, it is hard to tell whether or not the frequency content of a signal evolves over time, even though the phase of the Fourier transform relates to time shifting. On the other hand, except for a few special cases, the frequency content of the majority of signals encountered in the real world change with time. Recently, to overcome the problem that Fourier transform is unable to represent a nonstationary signal, time–frequency analysis methods that can simultaneously represent information about the time and frequency of a signal have been developed. In this study, the damage process of cross-ply carbon fiber reinforced plastics (CFRP) during a monotonic tensile test was characterized by acoustic emission (AE). Different laminated types of CFRP were used to determine the characteristics of the AE signal and frequency. The time–frequency analysis method was found to be useful for the determination of the fracture mechanism in CFRP (such as, matrix cracking, debonding– delamination, and fiber fracture). © 2003 Wiley Periodicals, Inc. J Appl Polym Sci 88: 1659–1664, 2003

Keywords: composites; failure

INTRODUCTION

The increasing use of composite materials in industry over the last three decades, particularly in safety critical structures such as primary and secondary aircraft components, has led to the development of ultrasonic nondestructive testing (NDT) techniques for detecting internal defects in composites. Since 1970, X-ray, ultrasonic C-scan, and acousto-ultrasonic techniques have been applied for recognizing the form or location of internal damage.[1–6] However, conventional ultrasonic techniques, such as the normal incidence pulse echo, have difficulty in identifying material internal defects (e.g., what caused the final fracture and how did the damage develop, material deformation, the detection of microscopic defects, dynamic fracture mechanics, etc.).

The structural failure of composites is a complicated process that is preceded by a sequence of microstructural damage. The composite structure sometimes fails catastrophically, without any apparent indication. Thus, two major requirements for the practical application of such composites is to ensure that the composites have structural reliability and to reveal the failure mechanisms of the composites. Matrix crack, fiber fracture, pull-out, delamination, and debonding are the most likely microfailure modes of the composites and serve as typical acoustic emission (AE) sources. Thus, AE testing should be a suitable method for investigating the entire failure process of the composites. In fact, AE monitoring of fiber-reinforced composite materials has been proven quite effective compared with other NDT methods.[7–9] To the authors' knowledge, however, many unsolved problems relating to analysis of fracture behavior remain unanswered because of the complex and anisotropic nature of the material.

The aim of this research was to analyze failure processes in fibrous composite materials, such as matrix cracking, fiber fracture, and failure of the fiber–matrix interface (delamination and debonding), using an AE method. Special types of specimens were made so that each fracture characteristic was expected and tested under tensile load. The AE signals generated during tensile load were recorded in real time, and the frequency ranges of the individual signals were examined by the time–frequency analysis method and classified based on spectral characteristics. This classification can be used to develop algorithms for autonomous health monitoring systems for composite structure.

EXPERIMENTAL

We tested unidirectional carbon–epoxy laminates that were made with prepreg (CU250NS, Hankuk Fiber Company). The laminates, $[90^{\circ}]_{16S}$, $[10^{\circ}]_{8S}$, and $[0°/90°]_{2S}$, were used under the same consolidation conditions [403 K (130°C) for 60 min under a pressure of

Correspondence to: K.-W. Nam (namkw@pknu.ac.kr).

Journal of Applied Polymer Science, Vol. 88, 1659–1664 (2003)

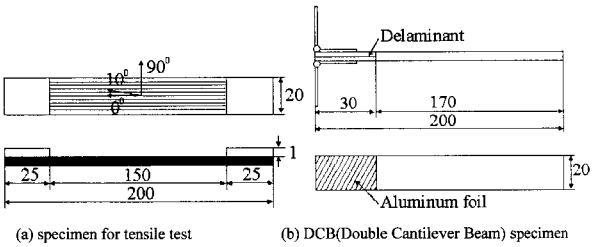

Figure 1 Dimensions of specimens; all dimensions in mm.

5.0 kgf/cm^2 for the first 10 min and then under a constant applied pressure of 1.0 kgf/cm^2 for the remaining 50 min]. The shapes and dimensions of the specimens are shown in Figure 1.

The AE measurements were carried out with a Mistras 2001 sensor (Physical Acoustic Corporation). The measurement systems are shown in Figure 2. The AE sensors were placed at equal distances of 25 mm from the center of the specimen (detail in Fig. 2). A PAC-R50 sensor was used for the AE count, and a broadband sensor with a reasonably flat response to ~1.0 MHz was used for frequency analysis. Two 40 dB preamplifiers with 30 kHz–2 MHz plug-in filters were used in these experiments. As is well known, signal discrimination in the presence of noise from a variety of sources is the most crucial problem in processing to gain the AE data during testing. Background noise during testing can be hydraulic, electrical, or mechanical. Various methods of noise suppression were considered and implemented. The grip sections of the specimens were covered with thin aluminum plates bonded by epoxy resin to reduce mechanical noise. Clay wrapped around the top and bottom sections of the specimens acted as an additional damper to eliminate noise produced by the environment. The tensile tests were performed at room temperature using a servo-hydraulic testing machine (Shimadzu model EHF-ED10) with a capacity of 0.98 MN and under a cross-head speed of 3 mm/min.

Failure process

Three main mechanisms of the microfailure caused in laminated composites are as follows:[10, 11] (1) Matrix

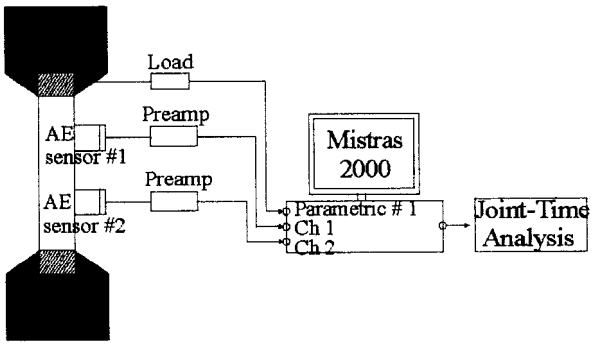

Figure 2 Schematic diagram of AE for monitoring of fracture mechanism in CFRP.

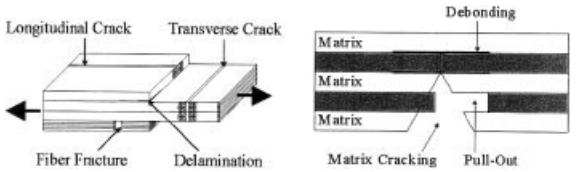

Figure 3 Schematic representation of the main macroscopic damage in CFRP.

cracking, which occurs both in the resin-rich part and at the points on the fiber layers that are oriented transversely to the perpendicular load in the laminated composites. The latter cracking, especially at low strain, is observed as transverse microcracks that appear on the surface of materials at regular intervals. (2) Failure of the fiber–matrix interface, which includes (a) the fiber–matrix debonding due to normal stress in the fiber, and (b) the local delamination at the inter-ply interface caused by straightening out fiber undulation in the straining longitudinal direction of the fiber. (3) Fiber breakage, which usually occurs in the case of fibers oriented perpendicular to the load. Transverse layers in the laminates are caused both by the misalignment of fibers and by initial defects during material handling in the fabrication process, and start at the early stage of deformation.

The typical failure process of fibrous composites just described is shown in Figure 3.

Short-time fourier transform

Because the classical Fourier transform analysis does not associate with any particular time, it does not explicitly reveal the time-varying nature of nonstationary signals. The most straightforward approach of characterizing the frequency of a signal as a function of time is to divide the signal into several overlapping blocks and carrying out the Fourier transform of each individual block of data. This process has become known as the short-time Fourier transform (STFT) and roughly reflects how the frequency content of a signal changes with time. The STFT process can be expressed by the following equation:

$$\mathrm{STFT}(t,\omega) = \int s(\tau)\gamma^*_{t,\omega}(\tau)d\tau = \int s(\tau)\gamma^*(\tau - t)e^{-j\omega\tau}d\tau \quad (1)$$

where t is time and ω is frequency. Equation 1 is a regular inner product and reflects the similarity between the signal $s(\tau)$ and the elementary function $\gamma(\tau - t)e^{-j\omega\tau}$ that are concentrated in both time and frequency domains. The function $\gamma(t)$ usually has a short time duration and it is therefore named the window function. The STFT spectrogram is the most simple and widely used time-dependent spectrum, which roughly depicts energy distribution of a signal in the

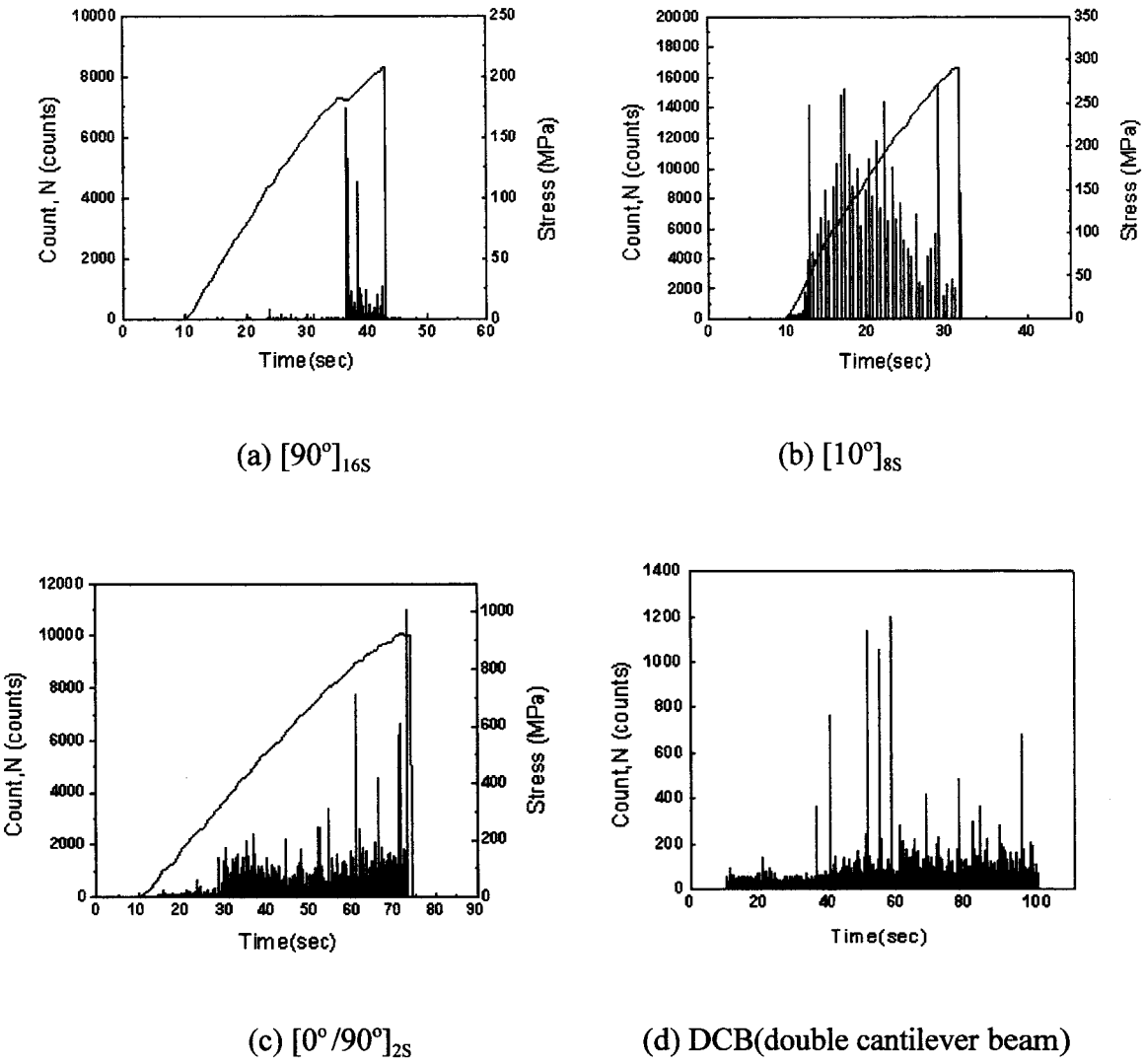

Figure 4 AE counts and stress versus time for constant strain rate loading.

joint time–frequency domain. The corresponding STFT spectrogram can be expressed by the following equation:

$$FS(t, \omega) = | \text{STFT}(t,\omega)|^2 \quad (2)$$

In this approach, the size of the blocks determines the time accuracy; that is, the smaller the block, the better the time resolution. However, frequency resolution is directly proportional to the size of the block. Thus, although a small block yields good time resolution, it deteriorates the frequency resolution and *vice versa* (the window effect).

RESULTS AND DISCUSSION

Load and AE count by time

A typical evolution of AE events and the stress and counts according to time are shown in Figure 4. In Figure 4(a), the $[90^\circ]_{16S}$ specimen was loaded perpendicular to the fiber direction. This specimen showed lower ultimate load and counts than those specimens shown in Figure 4(b) and 4(c).

In the $[90^\circ]_{16S}$ specimen, the main fracture mechanism was the failure of the matrix. In Figure 4(b), the $[10^\circ]_{8S}$ specimen was loaded with an incline of 10° to the fiber direction. This specimen showed higher ultimate load and counts than the $[90^\circ]_{16S}$ specimen. We considered that $[10^\circ]_{8S}$ specimen to have been loaded in shear because the fiber was arranged with an incline of 10° to the tensile direction. Therefore, the count shows a lot of evolution from the beginning stage.

The $[0^\circ/90^\circ]_{2S}$ specimen, was loaded parallel and perpendicular to the fiber direction, is shown in Figure 4(c). This specimen showed much higher ultimate load and counts than other ones because a mixed mode of failure occurred; that is, matrix cracking, failure of the fiber–matrix interface, and fiber break-

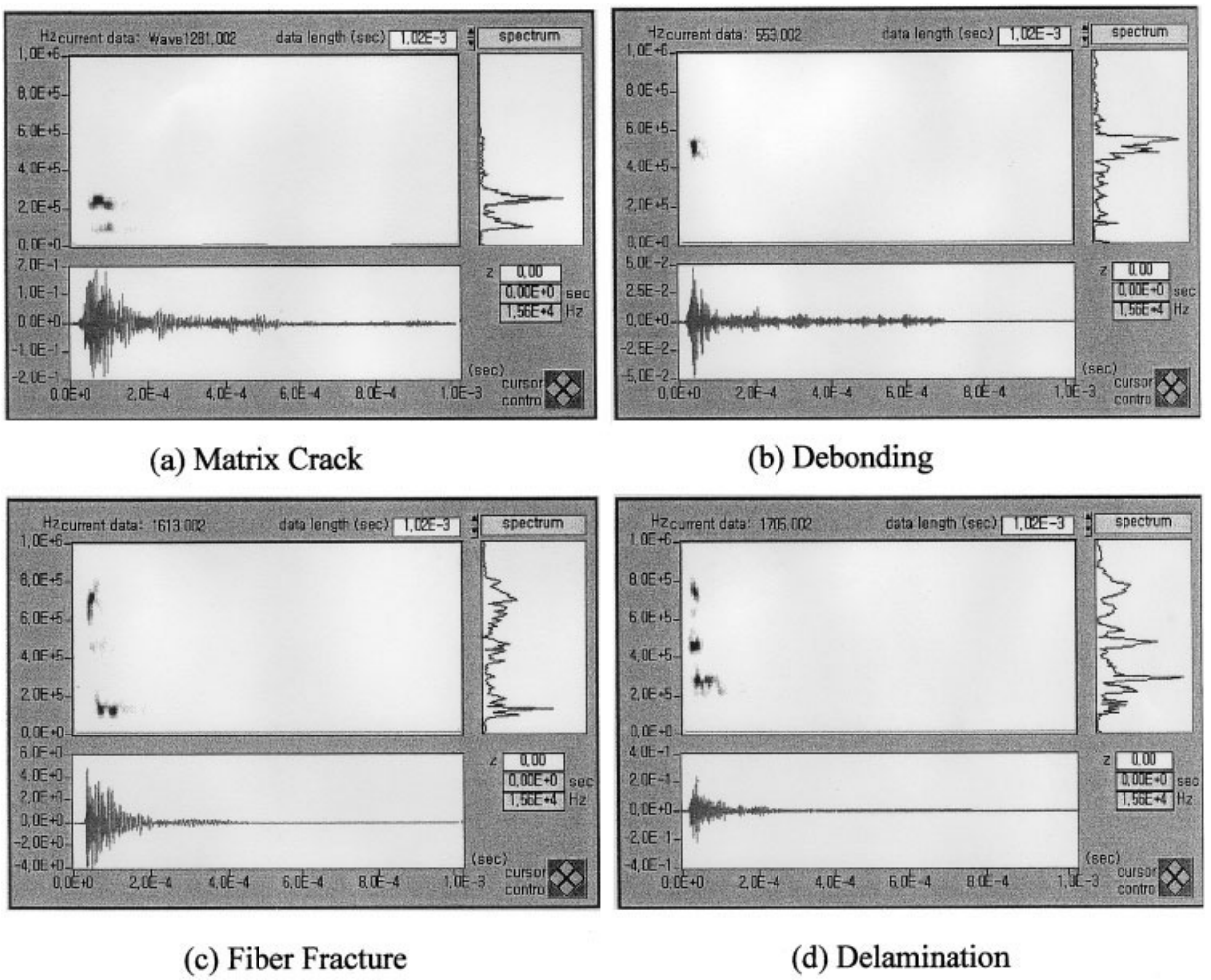

Figure 5 AE signal analysis results of fracture mechanism.

ing. The number of AE counts increased rapidly near the ultimate load. We can conclude that fiber breakage was the main fracture mechanism rather than matrix cracking and failure of the fiber–matrix interface. As shown in Figure 4(d), the DCB (double cantilever beam) specimen showed a much lower load. The AE count was distributed relatively equally as the crack propagated.

Time–frequency analysis

The results of the frequency analysis for each fracture mode are shown in Figure 5. Figure 5(a) was obtained from the $[90^{\circ}]_{16S}$ specimen, which was arranged with the fibers perpendicular to the load direction. This AE signal was generated quickly in Figure 4(a) by the time–frequency method. The main failure mode in the $[90^{\circ}]_{16S}$ specimen is matrix cracking, and these signals have a low frequency range of approximately 250 kHz. Figure 5(b) was obtained from the $[10^{\circ}]_{8S}$ specimen with an incline of 10° to the load direction. In this specimen, AE signals were generated by matrix crack and debonding, and scarcely anything was generated by fiber failure. The signals have a frequency range 250 and 500 kHz. It can be assumed that these signals are obtained from matrix crack and debonding, respectively. Figure 5(c) is obtained from the $[0°/90°]_{2S}$ specimen, which was loaded parallel and perpendicular to the fiber direction. This specimen showed a complex failure mode like as matrix crack, debonding, fiber fracture, etc. The frequency range of the fiber fracture was identified as the discrimination of that of matrix crack and debonding.

As shown in Figure 5(c), we can find that the main fracture source of the matrix was generated from the beginning of loading, and the counts were abruptly generated at the ultimate load. The frequency range of 700 kHz was identified as fiber fracture by the analysis of AE signals generated at the ultimate load. Figure 5(d) is the result of the DCB specimen and it is shown fracture mode of delamination. The frequency has dominant peaks at approximately 250, 500, and 700 kHz. As already mentioned, this is the same frequency range that is generated at matrix crack, debonding,

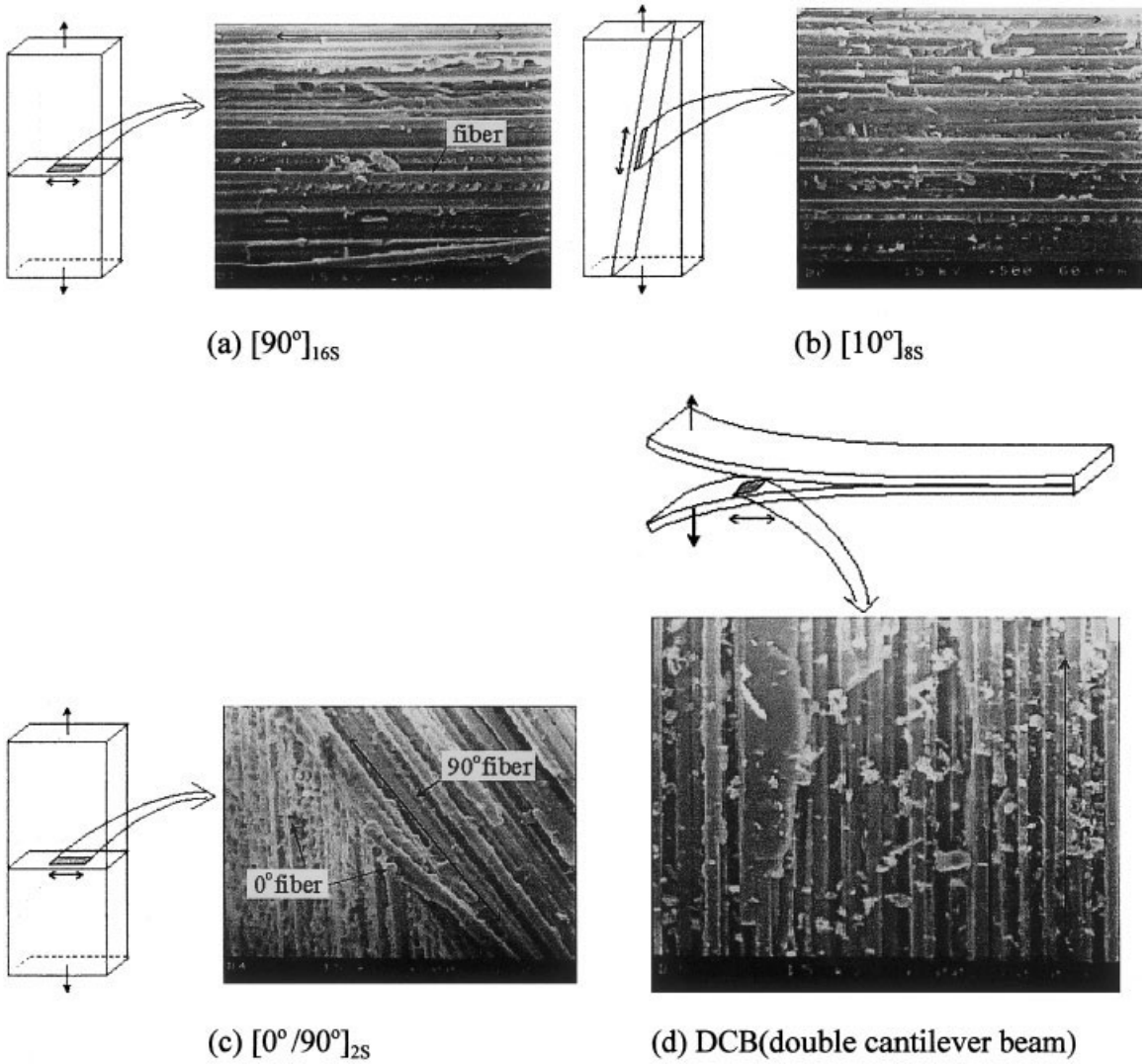

Figure 6 SEM fractographs showing the fracture surfaces (×500).

and fiber fracture. Therefore, it can be thought that the DCB specimen was generated all fracture modes at the same time.

Fractography

Four types of fracture surfaces were observed by scanning electron microscopic (SEM). The fracture surface of the $[90°]_{16S}$ specimen that was loaded perpendicular to the fiber direction is shown in Figure 6(a). The fracture occurs in the matrix. The results for $[10^{\circ}]_{8S}$ specimen, shown in Figure 6(b), was generated by debonding along the angle of fiber arrangement with shear stress. Figure 6(c), the results of $[0^{\circ}/90°]_{2S}$ specimen, shows matrix crack and debonding as well as fiber fracture. Figure 6(d) was obtained from DCB specimen and it shows the fracture surface of delamination. The cases illustrated in Figures (c) and (d) indicate that this specimen had complexly generated matrix crack, debonding, and fiber fracture.

CONCLUSIONS

The AE characteristics of CFRP were analyzed for four types of specimen. The main results are summarized as follows: The matrix crack has dominant peaks at the low frequency range of approximately 250 kHz. The debonding and fiber fracture events have dominant peaks at approximately 500 and 700 kHz, respectively. Matrix cracking, debonding, and fiber fracture were generated during the delamination that occurred in the composite materials. Based on the NDE analysis of AE signals by the time–frequency analysis method, it should also be possible to classify, in real time, the fracture mechanisms resulted from matrix crack, fail-

ure of the fiber–matrix interface (debonding and delamination), and fiber fracture.

REFERENCES

1. Fassbender, R.H.; Hagemaeier, D.J. Mater Eval 1983, 41(7), 831.
2. James, T.S.; Polansky, D.; Berger, H. NDT Int 1988, 21(4), 277.
3. Jones, T.S Mater Eval 1985, 43(6), 746.
4. Bar-Cohen, Y.; Crane, R.L. Mater Eval 1982, 40(9) 970.
5. Vary, A.; Lark, R.F. J Testing Eval 1979, 7(4), 185.
6. Talrefa, R. Acousto-Ultrasonics: Theory and Application; Duke, J.C., ed.; Plenum: New York, 1998, p. 191.
7. Caprino, G.; Teti, R. Compos Sci Technol 1995, 53,13.
8. Nam, K.W.; Ahn, S.H.; Lee, S.K.; Kim, H.S.; Moon, C.K. J Korean Soc Nondestructive Testing 2001, 21, 39 (in Korean).
9. Mizutani, Y.; Nagashima, K.; Takemoto, M. ACCM-1 1998, 645-1.
10. Sun, F.; Iwamoto, M.; Jinen, E.; Sizuki, M. J Soc Mat Sci, Jpn: Zairyo 1989, 38, 360 (in Japanese).
11. Uenoya, T. Progress in Acoustic Emission IV; Yamaguchi, K., et al., eds.; Japan Soc. NDI: Tokyo, 1988; p 679.